ELSEVIER

European Journal of Pharmaceutics and Biopharmaceutics 51 (2001) 249–257

European Journal of Pharmaceutics and Biopharmaceutics

www.elsevier.com/locate/ejphabio

Research paper

About the use of stoichiometric hydroxyapatite in compression – incidence of manufacturing process on compressibility

C. Pontier[a,b,*], M. Viana[a], E. Champion[b], D. Bernache-Assollant[b], D. Chulia[a]

[a]*Faculté de Pharmacie, Laboratoire de Pharmacie Galénique, G.E.F.So.D. E.A. 2631, Limoges, France*
[b]*Faculté des Sciences, S.P.C.T.S. UMR 6638, Limoges, France*

Received 3 October 2000; accepted in revised form 20 November 2000

Abstract

Literature concerning calcium phosphates in pharmacy exhibits the chemical diversity of the compounds available. Some excipient manufacturers offer hydroxyapatite as a direct compression excipient, but the chemical analysis of this compound usually shows a variability of the composition: the so-called materials can be hydroxyapatite or other calcium phosphates, uncalcined (i.e. with a low crystallinity) or calcined and well-crystallized hydroxyapatite. This study points out the incidence of the crystallinity of one compound (i.e. hydroxyapatite) on the mechanical properties. Stoichiometric hydroxyapatite is synthesized and compounds differing in their crystallinity, manufacturing process and particle size are manufactured. X-Ray diffraction analysis is used to investigate the chemical nature of the compounds. The mechanical study (study of the compression, diametral compressive strength, Heckel plots) highlights the negative effect of calcination on the mechanical properties. Porosity and specific surface area measurements show the effect of calcination on compaction. Uncalcined materials show bulk and mechanical properties in accordance with their use as direct compression excipients.

Keywords: Direct compression excipient; Stoichiometric hydroxyapatite; Calcination; Densification; Mechanical properties

1. Introduction

Direct compression is the most simple process to obtain tablets in pharmacy. It usually requires excipients that have been especially manufactured to have good flow and mechanical properties. Calcium phosphates can be used for this application, particularly due to their brittle behavior that generally provides highly resistant tablets [1]. The literature [1,2] points out that these compounds can have different chemical compositions defined by the ratio of the number of calcium (Ca) moles and the number of phosphorous (P) moles (Ca/P molar ratio). The different species can be dicalcium phosphate ($Ca_2(HPO_4)$, Ca/P $<$ 1.500), tricalcium phosphate ($Ca_3(PO_4)_2$, Ca/P $=$ 1.500), hydroxyapatite ($Ca_{10}(PO_4)_6(OH)_2$, Ca/P $=$ 1.667) or blends of these compounds (1.500 $<$ Ca/P $<$ 1.667). The purification method influences the properties and is usually not well-defined. Both the chemical nature and the production process can induce different compressibility behavior and a rationalization of the elaboration process of these compounds is then required.

In this paper, stoichiometric hydroxyapatite $Ca_{10}(PO_4)_6(OH)_2$ (Ca/P $=$ 1.667) has been studied to analyze the influence of the manufacturing processes such as the calcination (classically used as a purification method), the wet/dry granulation, and the particle size on the compressibility. This work is part of a larger study that evaluates the effect of the chemical composition (Ca/P molar ratio) on compressibility.

2. Materials and methods

2.1. Synthesis and manufacturing processes

The major steps of synthesis and manufacturing processes are shown in Fig. 1. Eight batches were studied: the abbreviations used to refer them and their manufacturing processes are summarized in Table 1.

Hydroxyapatite was prepared using a precipitation method of a diammonium phosphate (diammoniumhydrogenphosphate 99%, Sigma, Germany) on a calcium nitrate (tetrahydrate calcium nitrate 98%, Prolabo, France) under

* Corresponding author. G.E.F.So.D. E.A. 2631, Faculté de Pharmacie, Laboratoire de Pharmacie Galénique, 2, Rue du Docteur Marcland, 87025 Limoges Cedex, France. Tel.: +33-5-55-43-58-53; fax: +33-5-55-43-59-10.

E-mail address: catherine.pontier@unilim.fr (C. Pontier).

0939-6411/01/$ - see front matter
PII: S0939-6411(01)00137-0

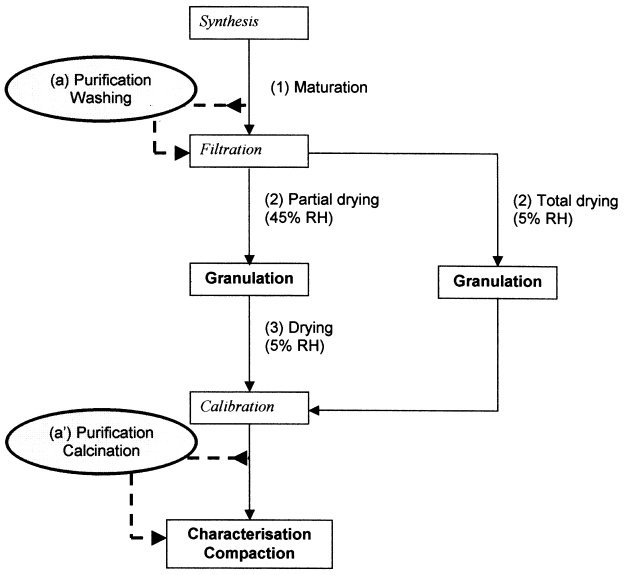

Fig. 1. Organigram of synthesis and manufacturing processes.

an argon atmosphere at regulated pH and temperature, as described elsewhere [3]. Reagent quantities, pH (9.5) and temperature (95°C) were adjusted to obtain compounds with a Ca/P molar ratio of 1.667. The precipitates were maintained in liquid suspension for a 7 day maturation at room temperature, without stirring, to reach the desired Ca/P molar ratio (step 1 in Fig. 1).

Filtration under vacuum was performed to obtain precipitates that were then dried (at a temperature of 60°C, Memmert, Schwabach, Germany) on thin layers (step 2) to reach a final moisture content of 5% (w/w) for the 'dry process', and of 45% (w/w) for the 'wet process'.

Granulation was performed using an oscillating granulator with a 2 mm screen (Erweka AR 400, Heusenstamm, Germany) without binder. Non-calibrated granules obtained by the wet process were dried in a fluidized bed (Glatt TR2, Haltingen-Binzen, Germany) for 10 min at 60°C (step 3) to reach the same final moisture content as the four dry-processed batches.

Two mean sizes of calibrated granules were studied: 200 μm, which is the most classical mean diameter for calcium phosphates used in direct compression [4], and 400 μm. The granules were obtained by a calibration step using a 315 and a 800 μm screen, respectively.

Two methods of purification were studied to eliminate the volatile nitrogenous synthesis residuals. Powders named 'uncalcined' were purified by washing the precipitates with 250 ml of distilled water during filtration. Materials named 'calcined' were purified by a 1 h calcination of the calibrated granules at 720°C (Kanthal Super, Rapid high temperature furnace, Bulten-Kanthal, Sweden).

Table 1
Manufacturing processes for the eight batches

Batch[a]	Wet/dry process	Granulation (mm)	Calibration (mm)	Purification method
W_{200uc}	W	2	0.315	Washing
W_{400uc}	W	2	0.800	Washing
D_{200uc}	D	2	0.315	Washing
D_{400uc}	D	2	0.800	Washing
W_{200c}	W	2	0.315	Washing
W_{400c}	W	2	0.800	Washing
D_{200c}	D	2	0.315	Washing
D_{400c}	D	2	0.800	Calcination

[a] W, wet process; D, dry process; 200, mean diameter = 200 μm; 400, mean diameter = 400 μm; c, calcined; uc, uncalcined.

2.2. Physicochemical characterizations

2.2.1. Chemical characterization

Powder X-ray diffraction (XRD) analysis was performed on the materials to determine their chemical nature.

The quantification of the chemical phases was performed according to the AFNOR S-94-066 standard [5]. After a 15 h calcination at 1000°C, calcium phosphates are constituted of two phases or less. If the Ca/P molar ratio of the material is lower than 1.667, it decomposes into β-tricalcium phosphate and hydroxyapatite, and if the Ca/P molar ratio is higher than 1.667, it decomposes into calcium oxide and hydroxyapatite.

XRD patterns were recorded with CuKα radiation on a $\theta/2\theta$ diffractometer (Siemens D5000, Germany) between 25 and 38° (2θ). The crystalline phases were deduced from a comparison of the registered patterns with the International Centre for Diffraction Data reference data file (PDF 9-432 for hydroxyapatite, PDF 9-169 for β-tricalcium phosphate and PDF 4-0777 for calcium oxide). For materials with a Ca/P molar ratio lower than 1.667, the rays chosen for the identification of the species are the rays corresponding to the (210) plane for hydroxyapatite ($2\theta = 31.8°$) and the (0.2.10) plane for β-tricalcium phosphate ($2\theta = 31°$). This method has been compared by other authors [6] to more classical identification and quantification methods and it has been shown to be more precise than chemical analysis (precision: 2.5 versus 0.5% for XRD). This technique has been coupled with infra-red spectroscopy to be sure of the absence of non-crystalline phases.

2.2.2. Specific surface area

Specific surface areas (m^2/g) of the powders were measured by low temperature helium adsorption using a Gemini 2360 Analyser (Micromeritics Instruments Inc., Norcross, GA) with liquid nitrogen as a cooler. Prior to adsorption measurements, the samples were degassed for 24 h at 80°C at a pressure lower than 4.10^{-2} Torr (VacPrep 61, Micromeritics Instruments Inc., Norcross, GA). The specific surface areas were calculated with the Brunauer–Emmett–Teller equation in the relative range of pressures of 0.05–0.30. Measurements were performed in triplicate.

2.2.3. Pycnometric density

Pycnometric densities (d_{pycno}) were measured in triplicate using a helium pycnometer (Accupyc 1330, Micromeritics Instruments Inc., Norcross, GA). The samples were dried 48 h at 80°C before the measurements.

2.2.4. Porosity

Porosity measurements were performed using a mercury intrusion porosimeter (Auto-Pore III, Micromeritics Instruments Inc., Norcross, GA) using pressures from 1 to 10^5 psi. The samples were dried 48 h before the measurements.

2.2.5. Particle size distribution

Particle size distribution was studied using 20 g of granules and a series of vibrating sieves from 56 to 1000 μm (Retsch AS 200 basic, Germany) according to the *European Pharmacopeia* procedure (2-9-12) [7]. The mean diameter (D_{50}, μm) was determined for each material. A dispersion coefficient was calculated as $(D_{25} - D_{75})/D_{50}$, where D_{25} and D_{75} are the theoretical diameters respectively rejecting 25 and 75% of the particles determined from the cumulative retained percent representation. Dispersion coefficients close to 1 characterize broad dispersions, and values close to 0 characterize narrow dispersions.

2.3. Powder bulk properties

The flowability was studied using a volumenometer (Model SVM2 unit, Erweka GmbH, Heusenstamm, Germany). The volume of 20 g of granules was determined after 0, 5, 10, 20, 30, 50, 100, 200, 300, 500, 750, 1000, 1250 and 1500 taps.

The bulk density (d_0, g/cm^3) was calculated according to Eq. (1).

$$d_0 = \frac{m}{V_0} = \frac{20}{V_0} \tag{1}$$

where V_0 (cm^3) is the initial volume of powder and m (g) is the mass of powder.

The compressibility factor (I_c, %) was determined using Eq. (2).

$$I_c = \left(1 - \frac{V_{1500}}{V_0}\right) \times 100 \tag{2}$$

where V_{1500} (ml) is the volume of the powder bed after 1500 taps.

The angle of repose of 10 g of powder was determined after flowing through a standardized funnel (2-9-16) [6].

2.4. Behavior under compression

The behavior of the different batches during compression was studied using an uniaxial press (Lloyd Instrument 6000R, Fareham, UK) with a 1 cm^3 cell (height = 10 mm, area = 10 mm^2) and flat punches. The cell was manually filled with an accurate mass of powder calculated from the bulk density. The inner surface of the cell was lubricated with a thin layer of magnesium stearate before filling. Pressures from 10 up to 300 MPa were used. The punch speed was 1.14 mm/min. The press was instrumented with an external extensometer (0–20 mm) and a force measuring sensor (0–30000 N) to accurately measure displacements and forces during compression and rupture tests. It was connected to a computer and the results were plotted using the R-Control software. Six compacts per pressure were manufactured.

2.4.1. Compressibility

Cycles of compression were studied as the evolution of the force (N) versus displacement (mm). The net compression work (NCW, J/g) was determined for each pressure of compaction as the area under the curve of the cycle of compression.

The packing coefficient (C_T, %) was determined according to Eq. (3).

$$C_T = \frac{H_0 - H_{0.5}}{H_0} \times 100 \tag{3}$$

where $H_{0.5}$ (mm) is the height of the powder bed for a pressure of compaction of 0.5 MPa, and H_0 (mm) is the initial height of the powder bed. C_T values lower than 25% characterize a good packing ability of the material [8].

The deformation mechanism was studied from the Heckel plots [9] using the Heckel equation (Eq. (4)) for the pressure of compaction 295 MPa.

$$-\ln\left(1 - \frac{d_{compact}}{d_{pycno}}\right) = KP + b \tag{4}$$

where $d_{compact}$ (g/cm^3) is the density of the compact, d_{pycno} (g/cm^3) is the pycnometric density of the powder, P (MPa) is the compaction pressure, and K and b are constants.

The mean yield pressure (P_y, MPa) was calculated for the pressure of compaction 295 MPa from the cycle of compression data. It was defined as the reciprocal of the slope of the linear part of the Heckel plots, corresponding to pressures of compaction between 70 and 150 MPa for the studied materials (i.e. 300 data points).

The P_y value is commonly used to investigate the mechanical behavior of materials: values lower than 100 MPa characterize plastic deformation and those higher than 100 MPa characterize brittle deformation.

The compaction ratio (%) was calculated using Eq. (5).

$$\text{Compaction ratio} = \frac{M/V}{d_{pycno}} \times 100 \tag{5}$$

where M is the mass of the compact (g), V is the volume of the compact after ejection (cm^3) and d_{pycno} is the pycnometric density (g/cm^3) of the materials.

2.4.2. Mechanical properties

Tensile strength (R_d, MPa) was determined by the diametral compressive test using the uniaxial Lloyd press and

calculated using Eq. (6).

$$R_d = \frac{2 \times F}{\pi \times D \times H} \quad (6)$$

where F (N) is the maximum diametral breaking force, D (mm) is the diameter of the compact and H (mm) is the height of the compact after ejection.

The compression range (MPa) was determined for each compound as the range of pressures allowing compacts removable from the die to be obtained.

3. Results

3.1. Physicochemical properties

3.1.1. Chemical composition

Patterns obtained according to the AFNOR standard (Fig. 2a) show that there is no characteristic peak of calcium oxide ($2\theta = 37.35°$) and no peak of β-tricalcium phosphate ($2\theta = 31°$). It is deduced from the AFNOR standard that the studied materials are pure hydroxyapatite with a Ca/P molar ratio of 1.667 ± 0.004.

The powder patterns show an apatitic structure. Materials that were purified by washing (W_{200uc}, W_{400uc}, D_{200uc} and D_{400uc}) showed a low crystallinity (Fig. 2b), and those that have been purified by heat (W_{200c}, W_{400c}, D_{200c} and D_{400c}) showed a higher crystallinity (Fig. 2c).

3.1.2. Specific surface area

Results are shown in Table 2. The granule size and the granulation process had no influence on specific surface area values. Uncalcined materials exhibited a high specific surface area (>40 m^2/g), whereas the thermal treatment dramatically decreased the surfaces (≈ 16 m^2/g). Raynaud et al. [10] described the evolution of the specific surface area of apatitic calcium phosphates versus the temperature of calcination. From 400 to 750°C, specific surface areas decrease due to a coalescence of the elementary particles without shrinkage.

3.1.3. Pycnometric density

Results of pycnometric density measurements are shown in Table 2. The values were independent of the granule size and the granulation process. Thermal treatment increased the values due to the improvement of the crystallinity and the coalescence of the elementary particles. All the values were lower than the theoretical density of hydroxyapatite (3.156 g/cm^3), signifying that the setting time and the temperature of the thermal treatment were not sufficient to reach a 100% crystallinity. The decrease of the pycnometric density from the theoretical density was 10 and 4% for uncalcined and calcined materials, respectively.

3.1.4. Porosity

Fig. 3a shows the porograms for calcined and uncalcined granules. In both cases, the different populations of pores were well-defined with two peaks of intrusion. Pore distribution only depended on thermal treatment. Porosimetry measurements performed on the granules did not show bed porosity, due to a close initial rearrangement. A first intrusion peak appeared around 70 μm corresponding to intergranular porosity. This value was slightly higher for calcined materials. In the case of uncalcined materials, the second peak corresponding to intragranular porosity was around 0.04 μm, whereas it was twice that for the calcined products (0.08 μm). Another interesting point to be noticed is the transformation of the bimodal intragranular porosity of the uncalcined materials (two mean diameters: 0.03 and 0.05 μm) into a monomodal pore distribution in the case of the calcined materials, suggesting that the thermal treatment

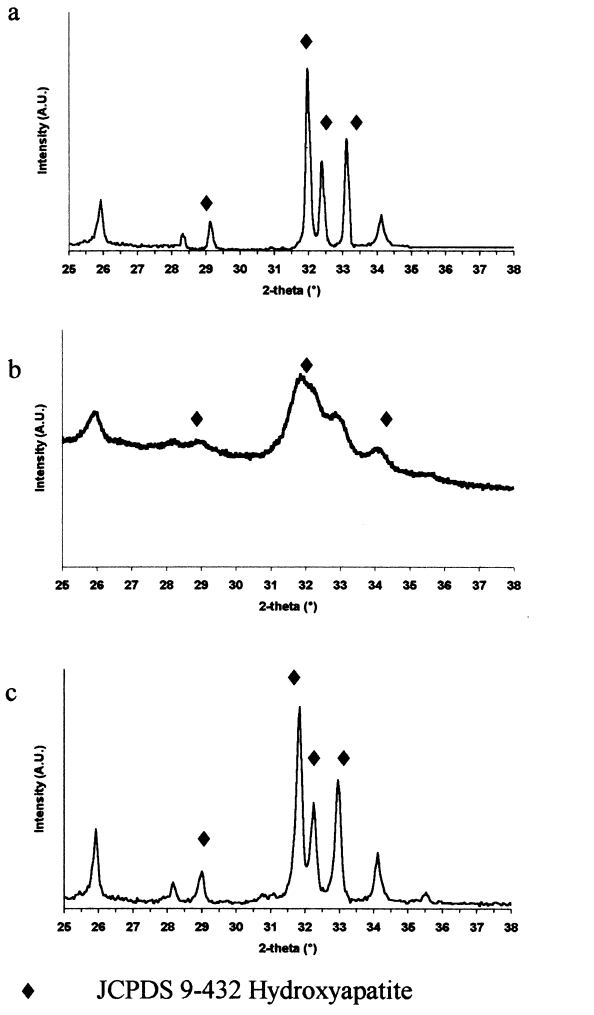

Fig. 2. Diffractograms of the materials to be compressed and the materials prepared according to the AFNOR standard.

Table 2
Physical and technological parameters[a]

Batch	Physical parameters		Technological parameters		
	Ss (m^2/g)	d_{pycno} (g/cm^3)	I_c (%)	α (°)	d_0 (g/cm^3)
W_{200uc}	46.0 ± 1.1	2.887 ± 0.002	18.5 ± 0.9	13.6 ± 0.8	0.58 ± 0.01
W_{400uc}	43.8 ± 1.4	2.847 ± 0.001	14.1 ± 3.2	9.4 ± 2.5	0.60 ± 0.02
D_{200uc}	44.6 ± 1.5	2.832 ± 0.000	20.4 ± 0.8	14.7 ± 0.7	0.52 ± 0.00
D_{400uc}	44.6 ± 2.2	2.786 ± 0.004	16.5 ± 1.4	11.3 ± 1.4	0.57 ± 0.01
W_{200c}	16.1 ± 0.1	3.004 ± 0.013	18.7 ± 1.5	10.5 ± 1.4	0.56 ± 0.01
W_{400c}	15.8 ± 0.1	3.013 ± 0.010	16.1 ± 2.1	12.3 ± 0.7	0.60 ± 0.01
D_{200c}	16.9 ± 0.3	3.027 ± 0.014	21.6 ± 0.4	13.0 ± 0.8	0.49 ± 0.00
D_{400c}	16.6 ± 0.3	3.025 ± 0.003	21.0 ± 0.4	11.9 ± 2.2	0.53 ± 0.03

[a] Ss, specific surface area (m^2/g); d_{pycno}, pycnometric density (g/cm^3); I_c, compressibility factor (%); α, angle of repose (°); d_0, bulk density (g/cm^3).

induced a coalescence of the micropores without modifying the global porosity.

Fig. 3b shows a comparison of the porograms obtained for the largest and the smallest particles. The intragranular porosity was not affected by the variation of the particle size. The mean diameter of the intergranular pores increased from 70 μm for the smallest particles to 150 μm for the coarsest particles.

3.1.5. Particle size distribution

The particle size distributions of the eight materials were monomodal. Fig. 4 shows an example of the particle size distribution for uncalcined and calcined materials. Particle size distributions of W_{200uc}, W_{200c}, D_{200uc} and D_{200c} were similar with mean diameters between 185 and 225 μm. W_{400uc}, W_{400c}, D_{400uc} and D_{400c} also had similar particle size distributions with mean diameters between 380 and 470 μm. Thermal treatment had no effect on the mean diameters and on the dispersion coefficients. This phenomenon is to be linked with the coalescence of the elementary particles at 720°C, without sintering (i.e. without any change in the global size of the granules). The dispersion coefficients were close to 0.59 for the powders with a mean diameter of 200 μm and 0.83 for the materials with a mean diameter of 400 μm, characterizing narrow particle size distributions in the first case and wider distributions for the coarsest particles.

3.2. Powder bulk properties

All the materials had good flow properties characterized by I_c values lower than 22% and angles of repose lower than 20° for all the batches (Table 2). The bulk powder properties seemed to be better for the largest particles (W_{400uc}, W_{400c}, D_{400uc} and D_{400c}) but the results obtained with the smallest granules indicated that no glidant would be required for their handling. Despite a larger porosity, the coarse materials exhibited a better packing ability.

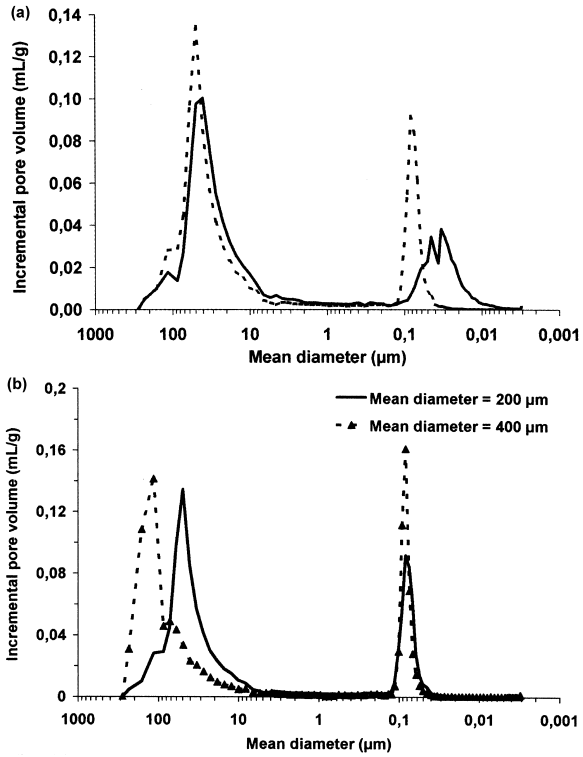

Fig. 3. (a) Effect of the thermal treatment on the pore size distribution. (b) Effect of the particle size on the pore size distribution.

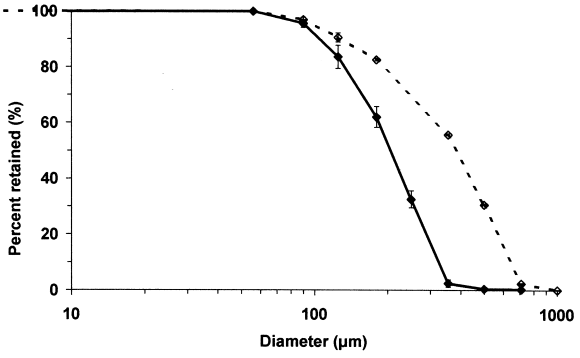

Fig. 4. Cumulative retained percent of materials with a mean diameter of 200 μm (solid line) and of 400 μm (broken line).

Table 3
Packing coefficient, mean yield pressures and compression range of the materials

Batch	C_T (%)	P_y (MPa)	Compression range (MPa)
W_{200uc}	29.7 ± 0.7	357	10–300
W_{400uc}	22.3 ± 0.9	342	10–300
D_{200uc}	34.4 ± 0.5	303	10–300
D_{400uc}	21.4 ± 0.8	317	10–300
W_{200c}	25.1 ± 0.5	500	50–100
W_{400c}	11.5 ± 0.9	455	50–100
D_{200c}	22.0 ± 0.4	390	50–100
D_{400c}	15.6 ± 0.4	435	50–100

3.3. Behavior under compression

Packing coefficients (C_T) were determined from the cycles of compression (Table 3). The packing coefficient was lower than 30% for the largest mean diameters, both for uncalcined and calcined materials, corresponding to a good packing ability of the materials. In the case of particles with a mean diameter of 200 μm, the C_T values were higher than 30%, and showed that the decrease of particle size had a negative effect on particle rearrangement under low pressure. However, these values were sufficient for a good filling of the compression cell. These results correlate with those obtained with the volumenometer, but the C_T values allowed a better discrimination than the I_c values. Comparison of results for W_{200uc} and W_{200c} on one hand, and for D_{200uc} and D_{200c} on the other hand showed that thermal treatment favorably influenced the packing ability of the materials. The same effect was observed for particles with a mean diameter of 400 μm. This phenomenon could be linked to the coalescence of the elementary particles due to calcination: the densification under low pressure will only concern the granules in the case of calcined materials, whereas it will concern both the granules and the elementary particles for the uncalcined materials.

Deformation of the materials was studied using Heckel plots. The P_y values are shown in Table 3. In all cases, the values were close to and higher than 400 MPa, corresponding to highly brittle compounds, as described in the literature [1]. Thermal treatment induced an increase of the mean yield pressure, which can indicate an increase of the fragmentary character due to calcination. The comparison of dry and wet processes showed that materials prepared according to the dry process had lower P_y values than the wet processed materials.

Whatever the material studied, the NCW increased linearly with the pressure of compaction as shown in Fig. 5. For the same pressure of compaction, the NCW used to compact calcined materials was twice that used for uncalcined materials in the case of particles with a mean diameter of 400 μm. The conversion of the energy received in compression work is more efficient in the case of the calcined materials. In the case of the 200 μm mean diameter, the difference due to calcination is less evident.

Evolution of the compaction ratios versus pressure of compaction is shown in Fig. 6. The comparison of the results for the uncalcined materials and the calcined materials showed that the compaction ratio depended neither on the particle size nor on the granulation process. Thermal treatment was the only parameter that appeared to have an

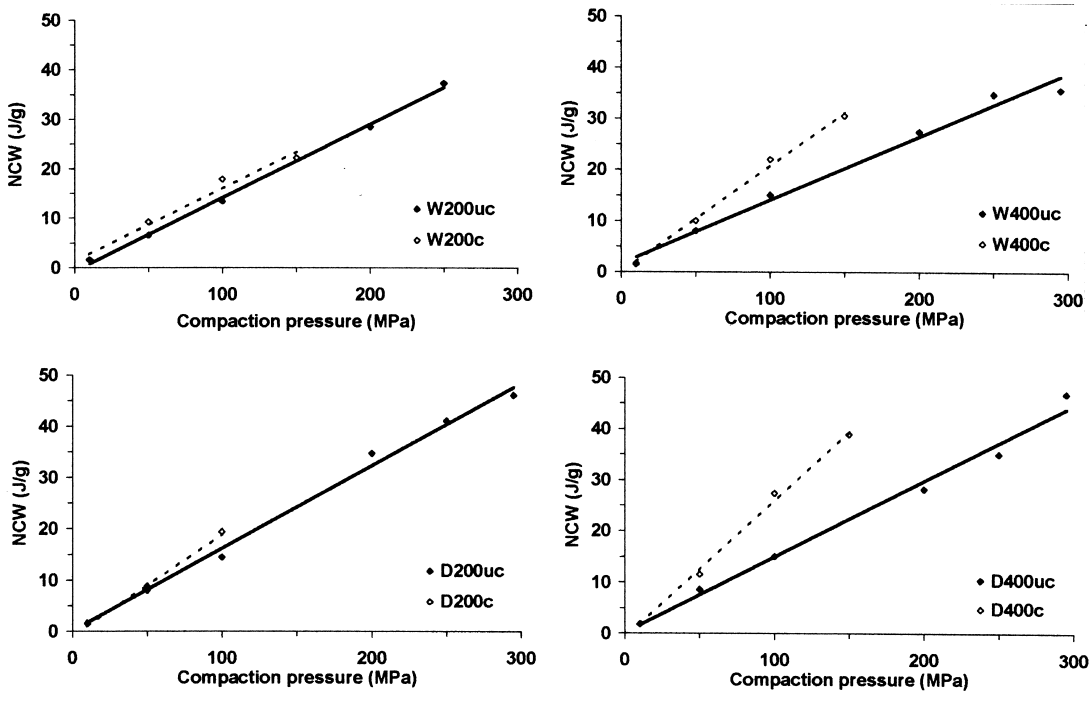

Fig. 5. Evolution of NCW versus pressure of compaction.

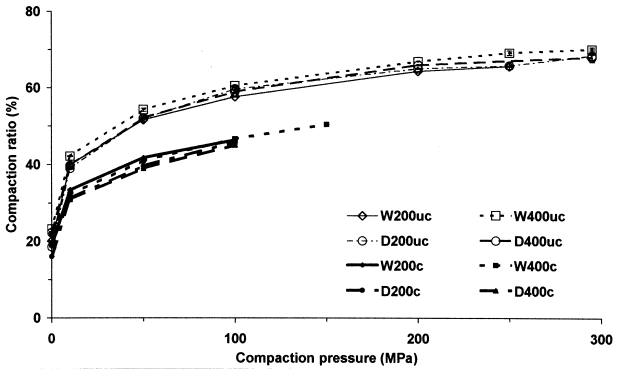

Fig. 6. Evolution of compaction ratio versus the pressure of compaction.

influence on the compaction ratio. The comparison of W_{200uc} and W_{200c}, which only differed in calcination, pointed out the decrease of the compaction ratio after thermal treatment. This decrease was about 10% for all the pressures when observing the four calcined compounds versus the uncalcined compounds.

Tensile strength measurements also showed the major effect of thermal treatment (Fig. 7). The manufacturing process and the particle size did not influence the material resistance. For D_{200uc} and D_{400uc}, internal lamination occurred for pressures higher than 200 MPa, which explains the decrease in the diametral compressive strength. For W_{200uc} and W_{400uc}, both the compaction ratio and the tensile strength increased up to 300 MPa, showing that the compression limit was not reached. The compression range of the different materials is shown in Table 3. For uncalcined materials, the first pressure allowing a compact to be obtained was 10 MPa, and the pressure range went up to 300 MPa, which was the limit of the press. The compression range of calcined products was limited to 50–100 MPa, with lamination and capping occurring for higher pressures. This narrow range makes calcined materials difficult to use. Cohesion of calcined products was low, even for the highest pressures of compaction. For the same pressure of compaction, compacts of uncalcined materials were five times more cohesive than those of calcined materials, and cohesion reached values around 3 MPa for the highest pressures. The difference in cohesion between calcined and uncalcined materials was not linked to the difference between compaction ratios. Fig. 8 shows that for the same compaction ratio, cohesion was twice as high for uncalcined materials. Comparison of the physical structure of the materials partially explains this phenomenon. Specific surface area measurements confirm this hypothesis: thermal treatment decreased the specific surface area of the powders and thus limited the contact surfaces available for the formation of bridges between granules that would ensure particle cohesion.

4. Discussion

Different manufacturing and purification processes have been compared to evaluate their impact on the technological properties and the compressibility of hydroxyapatite.

4.1. Physicochemical properties

The particle size distribution was influenced by the mechanical treatment (i.e. the size of the calibration screen) and not by the thermal treatment. The porosimetry study showed that the change in mean diameter only induced a change in the intergranular porosity. Porosimetry also points out that the thermal treatment influenced the pore size distribution by enhancing the intragranular pore size. The results obtained using these two methods of characterization are thus complementary in the study of the particle size distribution. The comparison with the results obtained by measuring the specific surface area explains these changes after thermal treatment. The calcination induced a coalescence of the elementary particles without shrinkage associated with a coalescence of the micropores in order to obtain larger pores. It induces a decrease of the specific surface areas after calcination without any change in the global porosity.

Whatever the manufacturing process ('wet' or 'dry' granulation) and the purification method (thermal treatment or washing of the precipitate), the flow properties of materials

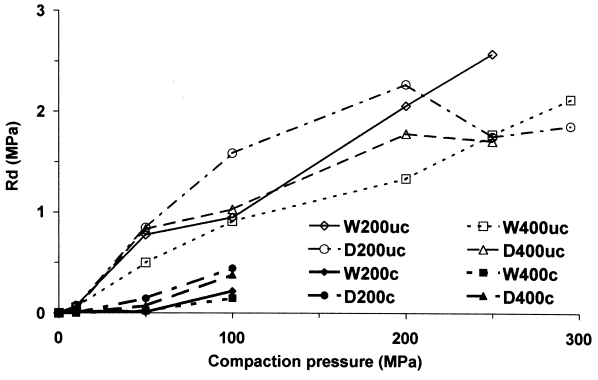

Fig. 7. Evolution of the tensile strength versus the compaction pressure and compression range.

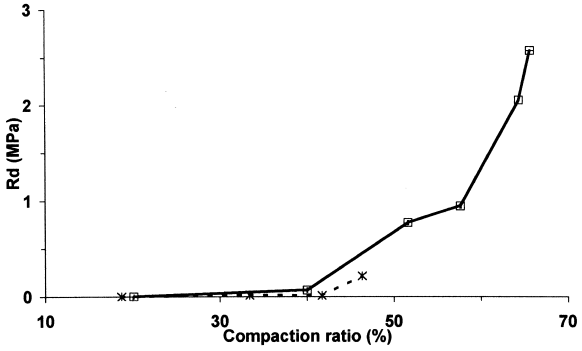

Fig. 8. Evolution of tensile strength versus the compaction ratio.

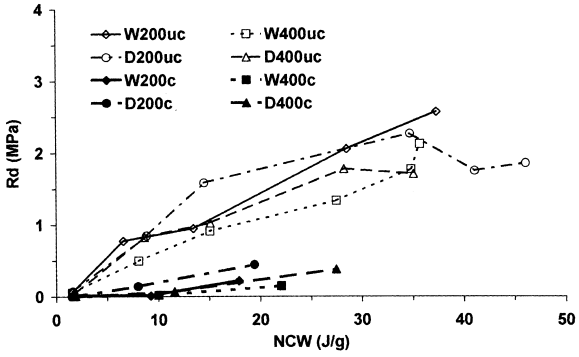

Fig. 9. Evolution of tensile strength versus the NCW.

were perfectly suited for use in direct compression. The 200 μm mean diameter induced a slight alteration of the flowing ability, but results were still compatible with a use in direct compression. Results of the porosimetry measurements explain those observations: the smallest particles exhibited small intergranular pores that were unfavorable to the powder flowability. This alteration is more evident when observing the C_T values: values obtained for W_{200uc}, D_{200uc}, W_{200c} and D_{200c} revealed an unfavorable powder flowability. The C_T values appear to be much more discriminating than the classical I_c and angle of repose.

4.2. Mechanical properties

Mechanical properties were highly dependent on the thermal treatment. Calcination is unfavorable to compression due to different effects. It restricted the handling ability of the materials by dramatically limiting their compression range (lower than 100 MPa versus 300 MPa for uncalcined materials), and reduced the compaction ratios. At the same time, even if the energy provided for compression seems to be better converted in compression work for the calcined materials, it is less converted into cohesion: for the same compression work, tensile strength can be up to ten times lower for calcined than for uncalcined materials (Fig. 9). The efficacy of compression is thus worse after thermal treatment, which is the most common purification method of apatitic calcium phosphates. A hypothesis to explain these observations is that the coalescence of the elementary particles due to calcination partly prevents the formation of bindings between the particles. The fragmentation is less important for the particles with a mean diameter of 200 μm due to their small size, and the NCW is then the same for calcined and uncalcined materials. These phenomena make calcined materials bad binders and they cannot be used as direct compression fillers, despite their good flow properties. Uncalcined materials can be compressed on a wide range of pressures, providing high compaction ratios and cohesive compacts. They have good rheological properties as well as good mechanical properties and can then be used as direct compression binders. Various particle sizes can be manufactured to be adapted to the granulometry of the other constituents of the formulation without impairing compressibility properties.

5. Conclusion

The aim of this study was to evaluate the impact of different purification methods (washing or calcination) and manufacturing processes on the compressibility of one chemical compound: hydroxyapatite. The manufacturing process (wet or dry granulation) and the particle size slightly influence the compressibility of hydroxyapatite: the particle size can be adapted to the granulometry of the other components of the formula without significant impairment of the flowability or the compressibility. Two particle sizes have been studied. This parameter only influences the flowing properties of the materials which remain favorable for the smallest sizes. Results also point out the incidence of the method of purification on the mechanical properties of the materials. The classical method which is a thermal treatment induces an important decrease of the mechanical properties. The washing of the precipitate is an efficient alternative to obtain pure materials with interesting mechanical properties. Further work concerning the blending ability and the lyoavailability (i.e. in vitro dissolution tests) will evaluate more precisely the impact of this factor.

On the basis of the results obtained with one chemical composition, it is suggested that the use of calcination as a method of purification is avoided. In the case of hydroxyapatite, calcination impairs mechanical properties and calcined materials will not be useful in compression. Uncalcined materials can be used as direct compression binders due to their satisfying flow and mechanical properties.

References

[1] P.-C. Schmidt, R. Herzog, Calcium phosphates in pharmaceutical tabletting. 2. Comparison of tabletting properties, Pharm. World Sci. 15 (1993) 116–122.
[2] L. Ertell, J.-T. Carstensen, Physical and chemical properties of calcium phosphates for solid-phase pharmaceutical formulations, Drug Dev. Ind. Pharm. 16 (1990) 1121–1133.
[3] M. Jarcho, C.-H. Bolen, M.-B. Thomas, J. Bobick, J.-F. Kay, R.-H. Doremus, Hydroxylapatite synthesis and characterization in dense polycrystalline form, J. Mat. Sci. 11 (1976) 2027–2035.
[4] Tribasic calcium phosphate, in: A. Wade, P.J. Weller (Eds.), Handbook of Pharmaceutical Excipients, 2nd Edition, The Pharmaceutical Press, London, 1994, pp. 61–62.
[5] Matériaux pour implants chirurgicaux, Détermination quantitative du rapport Ca/P de phosphates de calcium, AFNOR S-94-066, 1998.
[6] S. Raynaud, E. Champion, D. Bernache-Assollant, J.-P. Laval, Determination of calcium/phosphorous atomic ratio of calcium phosphate apatites using X-ray diffractometry, J. Am. Ceram. Soc. 84 (2001) 359–366.
[7] European Pharmacopeia, 3rd Edition, Council of Europe, Strasbourg, 1997.
[8] C.-M.-D. Gabaude, J.-C. Gautier, Ph. Saudemon, D. Chulia, Validation of a new pertinent packing coefficient to estimate flow properties of pharmaceutical powders at a very early development stage, by

comparison with mercury intrusion and classical flowability methods, J. Mat. Sci. 36 (2001) 1–11.
[9] R.-W. Heckel, Density-pressure relationships in powder compaction, Trans. Met. Soc. AIME 221 (1961) 671–675.
[10] S. Raynaud, E. Champion, D. Bernache-Assollant, Synthesis, sintering and mechanical characteristics of non-stoichiometric apatite ceramics, 11th International Symposium on Ceramics in Medicine (New York), Bioceramics 11 (1998) 109–112.